Journal of Cosmetics, Dermatological Sciences and Applications, 2024, 14, 12-28
https://www.scirp.org/journal/jcdsa
ISSN Online: 2161-4512
ISSN Print: 2161-4105

Quantification of *In Vivo* Epidermal Keratinocyte Architecture Associated with the Signs of Skin Aging and the Skin Benefit Evaluation by Application of *Galactomyces* Ferment Filtrate (Pitera)-Containing Skin Care Product

Kukizo Miyamoto[1*], Yoko Munakata[1], Keisuke Fujii[1], Chenlu Lei[1], Ley Yang[2], Suda Sudarsana[1], Masutaka Furue[3]

[1]Research and Development, Kobe Innovation Center, Procter and Gamble Innovation GK, Kobe, Japan
[2]Global Scientific Communications, P & G Guangzhou Ltd., Guangzhou, China
[3]Department of Dermatology, Graduate School of Medical Sciences, Kyushu University, Fukuoka, Japan
Email: *miyamoto.ku@pg.com

How to cite this paper: Miyamoto, K., Munakata, Y., Fujii, K., Lei, C.L., Yang, L., Sudarsana, S. and Furue, M. (2024) Quantification of *In Vivo* Epidermal Keratinocyte Architecture Associated with the Signs of Skin Aging and the Skin Benefit Evaluation by Application of *Galactomyces* Ferment Filtrate (Pitera)-Containing Skin Care Product. *Journal of Cosmetics, Dermatological Sciences and Applications*, **14**, 12-28.
https://doi.org/10.4236/jcdsa.2024.141002

Received: January 20, 2023
Accepted: March 9, 2024
Published: March 12, 2024

Abstract

Background: Aged skin exhibits visual alterations such as wrinkles, rough texture, pore dilation, and dull skin tone, as well as physiological aging, namely, decreased hydration and increased transepidermal water loss (TEWL). Recent advances in coherence tomography have also revealed that skin aging affects *in vivo* epidermal keratinocyte architecture. However, the interconnectivity between spatial architectural aging and visual/physiological aging parameters remains largely unknown. **Purpose:** To elucidate whether the tomographic keratinocyte architectural aging is correlated with visual and physiological skin aging parameters and to quantitatively evaluate the improvements of the architectural, visual, and physiological aging parameters by the daily treatment of the skin care formula containing Galactomyces Ferment Filtrate (GFF, 8X Pitera™). **Method:** We measured the *in vivo* keratinocyte cellular architecture with two-photon stereoscopic tomography obtaining by-layer epidermal section images in 78 Asian females of various ages. Visual aging parameters were analyzed using a portable image capture system. Hydration and TEWL were also assessed. The anti-aging effects of GFF-containing skin moisturizer (SK-II LXP Cream™) were also examined in two studies after twice-daily application for 2 (N = 35) and 4 (N = 32) weeks. **Results:** As for the keratinocyte cellular architecture, skin aging was significantly associated with decreased cell density and increased cell uniformity. These architectural aging parameters were significantly correlated with

visual and physiological aging parameters, namely, rough texture, wrinkles, pore dilation, dull skin tone, dehydration, and increased TEWL. The strong interconnectivity allowed us to develop formulae to estimate the keratinocyte architecture from visual aging parameters. Moreover, twice-daily application of SK-II significantly improved the keratinocyte architecture associated with multiple skin aging visual and physiological parameters. **Conclusion**: Skin aging is a process involving mutual interconnections among epidermal keratinocyte cellular architecture, visual, and physiological parameters. The GFF-containing moisturizer SK-II effectively improves spatial architecture of keratinocytes in epidermis and these evaluated skin aging parameters in a new trajectory over the course of treatment.

Keywords

Facial Skin Aging, *In Vivo* Keratinocyte Cellular Architecture, Visual Aging Parameter, Dehydration, Interconnectivity, New Trajectory, Galactomyces Ferment Filtrate, Pitera™, SK-II LXP Cream™

1. Introduction

Facial skin aging is a psycho-physical and social concern in humans. Biopsied skin samples show that skin aging is associated with epidermal thinning and flattening of the dermal-epidermal junction as well as the loss of collagen and elastin [1]. Recent technical advances in optical coherence tomography enable us to assess the *in vivo* architecture of epidermal cells. This noninvasive approach reveals that the size of epidermal keratinocytes continues to increase with age *in vivo* [2].

In addition to the above-mentioned microscopic morphological structure, facial skin aging generally affects macroscopic visual images. Facial skin aging is significantly associated with increases in wrinkles, texture, and pore size, while skin tone (L-value) decreases with age [3]-[9]. Facial skin aging is also associated with physiological alterations such as decreased skin hydration and increased transepidermal water loss (TEWL) [7] [9]. However, to the best of our knowledge, no studies have investigated the interconnectivity between visual/physiological alterations and *in vivo* cellular architectural aging.

SK-II LXP Cream™ (hereafter SK-II) contains *Galactomyces* ferment filtrate (GFF 8X Pitera™), which is a potent antioxidative agonist for aryl hydrocarbon receptor [10] [11]. GFF is known to increase the expression of filaggrin, caspase-14, and claudin-1, which may facilitate the production of natural moisturizing factors and strengthen the epidermal tight junction structure [10] [12] [13]. In addition, GFF inhibits oxidative stress mediated by proinflammatory cytokines in epidermal keratinocytes [11] [14]. In parallel with this in vitro evidence, several clinical studies have revealed that the daily application of GFF-containing moisturizer indeed increases facial skin hydration [9] [15] [16]. It also improves mask-induced skin damage [16] and potently reverses the facial

visual skin aging parameters [9]. However, it remains unknown whether this moisturizer affects the *in vivo* keratinocyte tomographic architecture.

In this study, our three-dimensional tomographic analysis demonstrated that facial skin aging decreased keratinocyte cellular density and increased its cellular uniformity. In addition, the tomographic keratinocyte architecture was significantly correlated with each visual aging parameter, namely, rough texture, wrinkles, pore dilation, and decreased L-value, as well as with dehydration parameters. The highly significant relationship among visual aging parameters and tomographic architecture allowed us to estimate the *in vivo* cellular architecture from visual parameters. Moreover, topical treatment with SK-II could rejuvenate the tomographic keratinocyte architecture in parallel with improvement of visual and physiological aging parameters.

2. Materials and Methods

2.1. Study Design

Skin evaluations were composed of three parts as follows: Study 1: basic skin research for understanding the relationship between epidermal keratinocyte architecture and visual/physiological properties of skin aging, Study 2: evaluation of SK-II's effects on tomographic keratinocyte architecture, and Study 3: evaluation of SK-II's effects on the visual and physiological aging parameters as well as estimated cellular architecture.

In Study 1 (Protocol CT12002), we measured epidermal keratinocyte architecture (cellular density and cellular uniformity), visual aging parameters (texture, wrinkles, pores, and L value), and physiological properties (hydration and TEWL) in 78 Asian females (age 21 - 69, mean ± SD: 43.97 ± 13.64). The epidermal architecture was assessed using *in vivo* two-photon stereoscopic tomography obtaining by-layer epidermal section images (DermaInspect MPTflex™ 10; JenLab GmbH, Jena, Germany). Skin hydration was measured with a Corneometer® CM825 (Courage + Khazaka, Courage + Khazaka Electronic GmbH, Cologne, Germany) and TEWL was assessed with a Vapometer® (Delphine Technologies Ltd., Kuopio, Finland).

Study 2 (Protocol CT12006) was performed to evaluate whether SK-II affects the epidermal keratinocyte architecture as well as skin hydration and TEWL in 32 Asian female volunteers aged 24 - 58 (41.3 ± 11.34). SK-II was applied twice daily to the left forearm in a 3 × 3 cm square area. The right forearm was not treated during the course of the study, and served as a control in order to compare the treatment site. Skin measurements were performed in both forearms at the start of the day (baseline), on days 14 and 28.

In Study 3 (Protocol CT23002), we assessed the effects of SK-II on various skin aging parameters in facial skin. Skin hydration, visual parameters, and estimated cellular architecture were measured in 35 Asian females aged 20 - 50 (35.1 ± 6.5). SK-II was applied on the subject's face twice daily and skin measurement was conducted at baseline (day 0) and on days 3, 7, and 14.

All study protocols were approved by the Ethical Committee of Global Product Stewardship in P&G Innovation Godo Kaisha. Written informed consent was obtained from all subjects prior to their enrollment in each study.

2.2. *In Vivo* Two-Photon Tomography for Cellular Density and Uniformity

The keratinocyte cellular architecture was examined using *in vivo* two-photon tomography with a DermaInspect MPTflex™ 10 (**Figure 1**) [17] [18]. This instrument allows 3D imaging with high spatial resolution in the submicrometer range based on two-photon excited fluorescence and second harmonic generation. Three repeated measurements were performed at the middle of the cheek on the left side of the face, or inner forearm. A combination of intense 80-MHz femtosecond near-infrared laser pulses and flying spot technology for beam scanning allowed imaging with high spatial and temporal resolution to be obtained. Light intensities in the range from MW·cm^{-2} to GW·cm^{-2} allowed the detection of endogenous fluorophores, targeting keratinocyte architecture in the granular layer of the skin, through two-photon excitation. The laser beam scanned a skin field of interest of a size of 300 × 300 lm^2 (512 × 512 pixels) with a typical beam well time of <40 μs per pixel, scanning at 2 lm pitch by depth, on

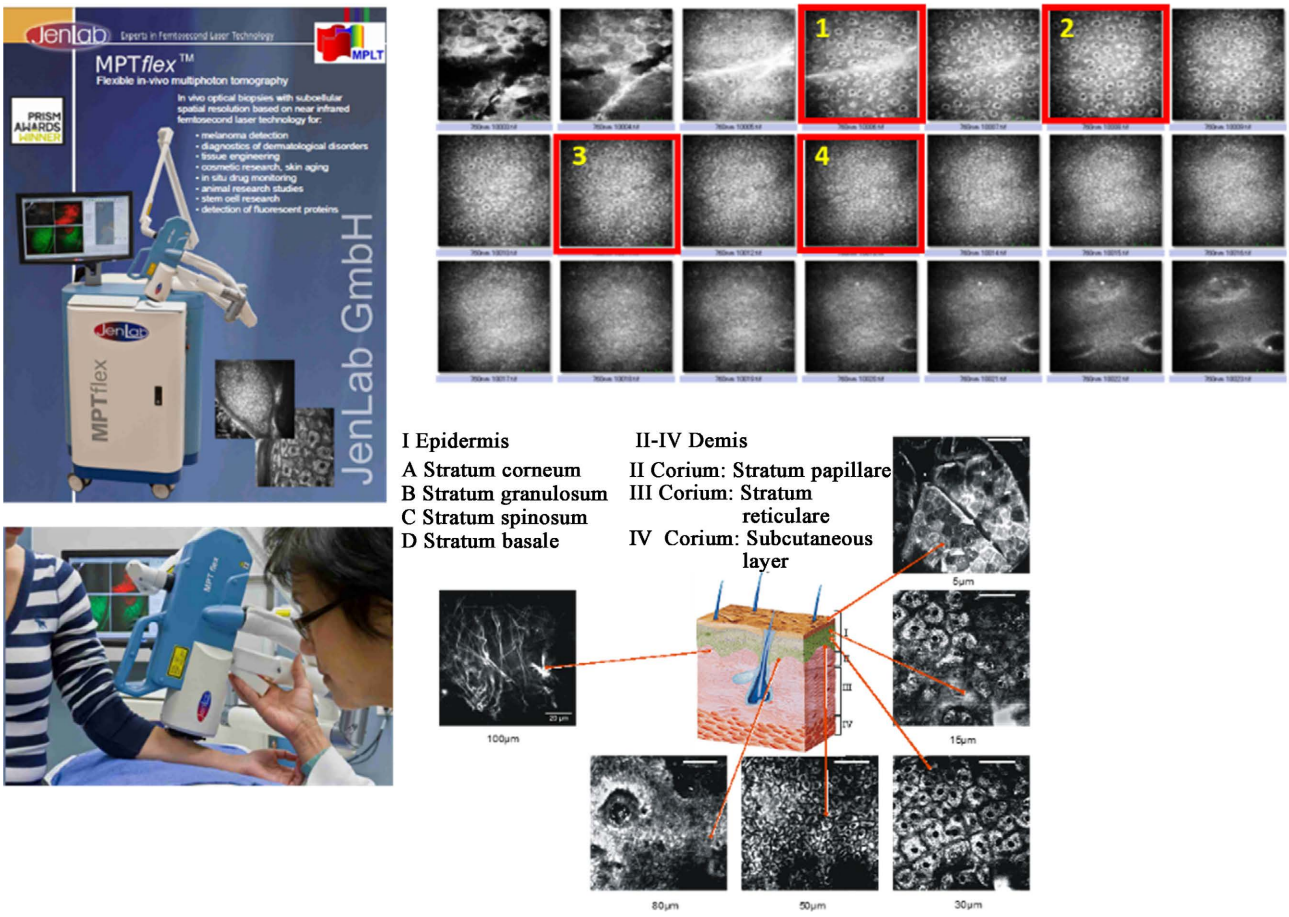

Figure 1. *In vivo* two-photon multiphoton tomography with DermaInspect MPTflex™ 10.

the skin of the cheek or forearm. The time between two laser pulses was 12 ns. The weak fluorescence was detected by sensitive photodetectors. Image processing was performed to obtain high-resolution autofluorescence images.

To quantify the keratinocyte architecture, we collected four layers of keratinocyte cellular images at 8 μm pitch (32 μm depth) at the central field of 100 × 100 μm in the epidermis layer below the stratum corneum (Figure 2). The cellular density was calculated using an image analysis algorithm. Meanwhile, the cellular uniformity was calculated using the following formula.

$$U_{shape} = \left(\sum_{i=1}^{m} \left(X_m - \frac{\overline{X}_i + \overline{Y}_i}{2} \right)^2 + \sum_{i=1}^{m} \left(Y_m - \frac{\overline{X}_i + \overline{Y}_i}{2} \right)^2 \right) \Big/ m$$

$$U_{size} = \left(\sum_{i=1}^{m} \left(X_m - \overline{X}_i \right)^2 + \sum_{i=1}^{m} \left(Y_m - \overline{Y}_i \right)^2 \right) \Big/ m$$

$$\text{Cellular Uniformity} = U_{shape} + U_{Size}$$

m: cell count, xi: short diameter of the cell, Y_i: long diameter of the cell

2.3. Facial Visual Aging Parameters

The subjects washed their faces using the prescribed cleansing foam and then spent 20 min acclimating to the environment of the measurement room. The examination room was maintained at a constant temperature and humidity (room temperature 20˚C ± 2˚C, relative humidity 50% ± 5%). None of the subjects underwent any type of esthetic treatment such as laser cosmetic procedures during the study period. Each subject's face was photographed using a portable image capture system (Magic Scan) illuminated by a number of 5600-K light-emitting diodes mounted at both left and right sides of the system (Figure 3) [9]. A high-resolution complementary-symmetry metal–oxide–semiconductor digital camera, capable of generating 1980 (vertical) × 1024 (horizontal) effective picture elements (pixels), was also mounted in the imaging module. A series of deep-learning-based post-calibration algorithms was carried out to adjust to the consistent brightness, hue, and saturation after capturing the facial images. This

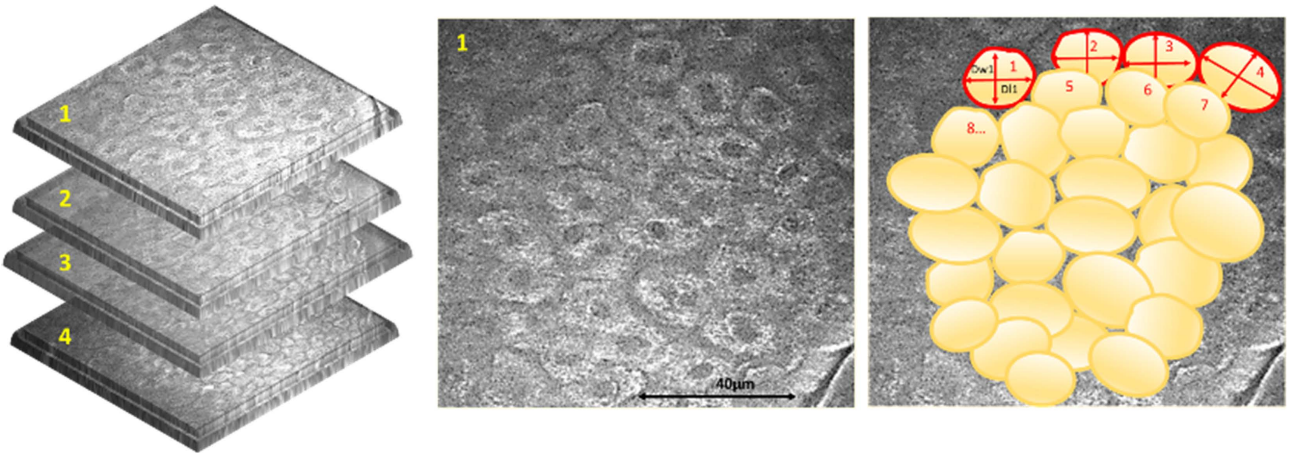

Figure 2. Selected two-photon images.

Figure 3. Magic Scan facial imaging system. Each subject's face was photographed using Magic Scan.

enabled the captured images to be controlled to ensure reproducible collection under the different external optical conditions. A neutral 8.0 gray color board (GretagMacbeth GmbH, Munich, Germany) was used for white balancing of the camera.

2.4. Objective Image Analysis for Texture, Wrinkles, Pores, and L Value

The region of interest (ROI) of the images was from the outer edge of the eye to the cheek, and the following characteristic objects were extracted by measuring the contrast in the shape and pixels using an image analysis algorithm [15] [16]. Wrinkles were defined as ≥5 mm in length, perimeter/length ratio ≤ 2.5, and circularity (perimeter^2/area) ≥ 34. Total wrinkle area fraction was quantified as follows: total wrinkle area (pixels)/ROI (pixels). As an index of texture, total texture area fraction [total texture area (pixels)/ROI (pixels)] was quantified as ≤ 3 mm^2 in area, aspect ratio ranging from 0.5 to 2, and color contrast deltaE ≥ 1.5. Facial skin tone (L-value) was also measured in the ROI. Pores were identified in an image analysis algorithm by detecting circular pore-like shapes via edge-enhanced binary images at the cheek region. The total area of detected pores was then calculated.

2.5. Statistical Analysis

All statistical analyses were performed using JMP® Pro 16.1.0 (SAS Institute Inc., Cary, NC, USA). For each outcome variable, data were analyzed by fitting a linear mixed-effects model with timepoint as the fixed effect and subject as the random effect to account for within-subject variation. Pearson's correlation coefficients (r) between the following variables were examined: 1: between skin cellular density and chronological age, skin hydration, TEWL, and four skin visual parameters (texture, wrinkles, pores, and L value) in Study 1. Quantitative comparisons were also performed for the following variables: 1: cellular density, cellular uniformity, hydration, TEWL, and visual parameters (texture, wrinkles,

pores, and L value) at the baseline versus at week 2 and week 4, upon treatment with SK-II in Study 2; and 2: those skin parameters at the baseline versus on days 3, 7, and 14 after the SK-II treatment in Study 3 using two-way ANOVA. Logistic regression analysis was performed to model the association of cell density and uniformity as response variables, and signs of skin aging parameters [texture, pores, wrinkles, and skin tone (L-value)] as exploratory variables. A P-value less than 0.05 was considered to be statistically significant.

3. Results

3.1. Tomographic Epidermal Keratinocyte Architecture is Correlated with Visual/Physiological Skin Aging Parameters

We measured tomographic architecture, visual, and physiological skin aging parameters in 78 women of various ages. A significant decrease in skin cellular density was observed in association with increasing age ($r = -0.289$, $P < 0.05$) (Figure 4(A)), while the cellular uniformity significantly increased with age ($r = 0.190$, $P < 0.05$) (Figure 4(B)). Facial skin aging was also significantly correlated with decreased hydration (Figure 4(C)) and increased TEWL (Figure 4(D)). Example images of facial skin and tomographic keratinocyte architecture at younger, middle, and older ages are shown in Figure 5.

As has been reported previously [3-9], facial skin aging was significantly associated with rough texture (Figure 6(A)), wrinkles (Figure 6(B)), pore dilation (Figure 6(C)), and decreased L value (Figure 6(D)).

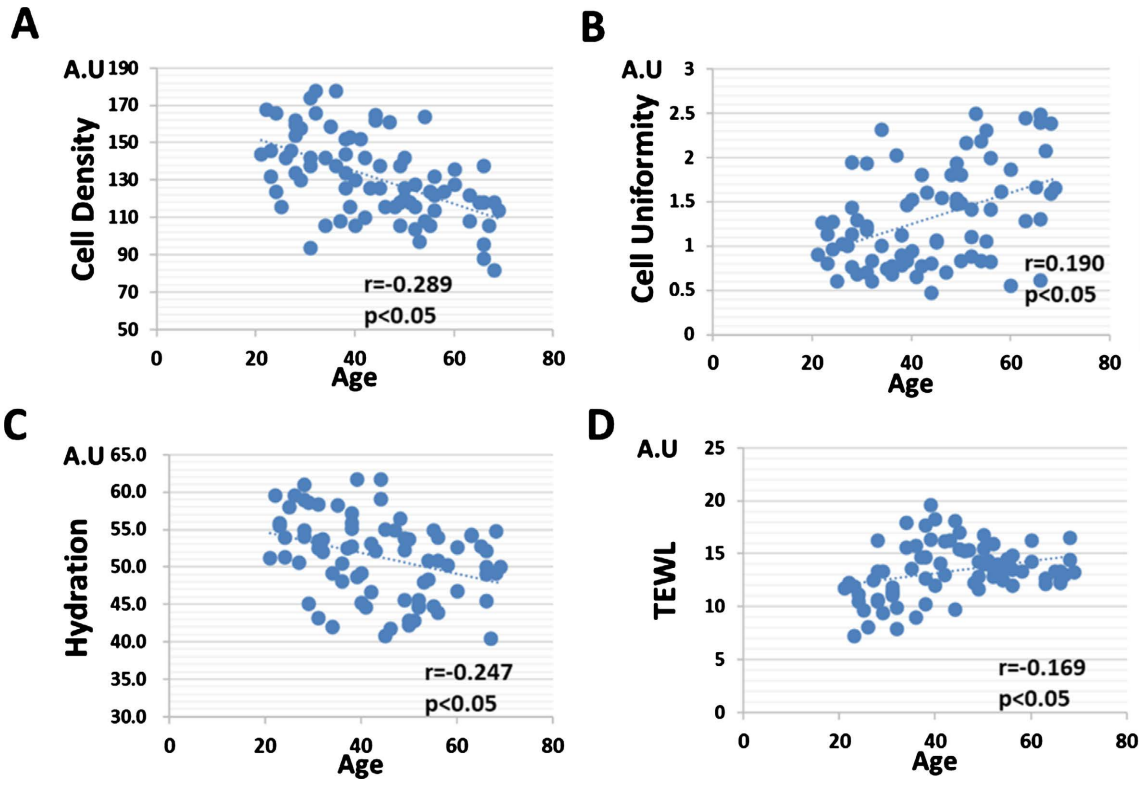

Figure 4. Age-related alterations of cell density (A), cell uniformity (B), hydration (C), and TEWL (D).

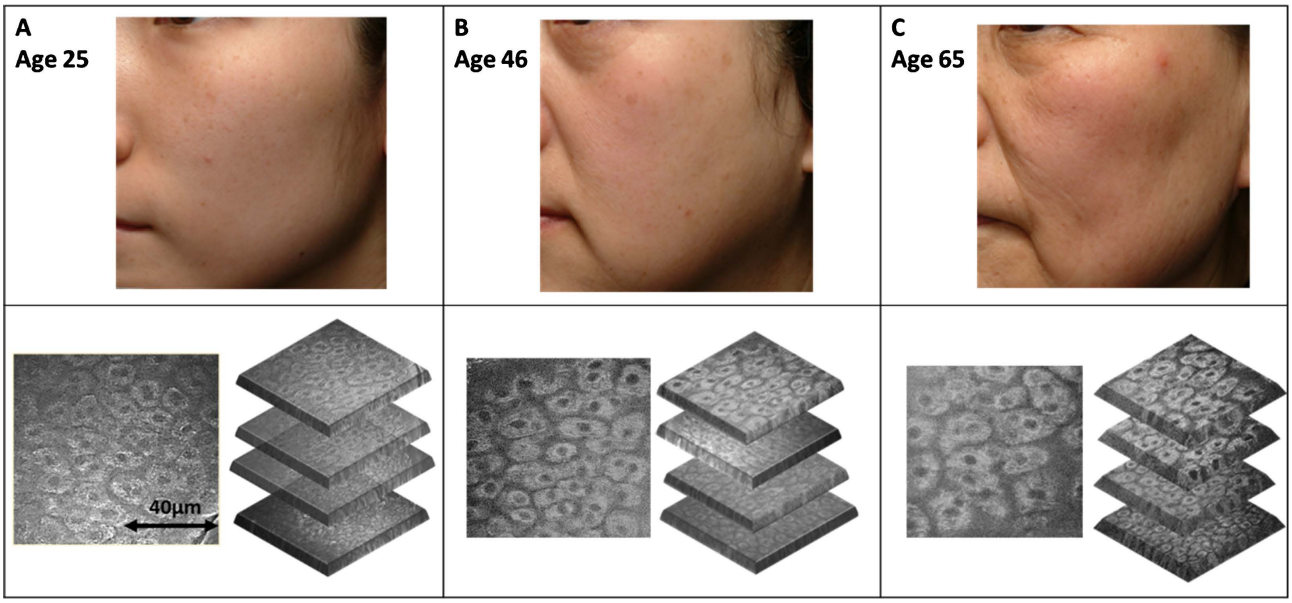

Figure 5. Examples of facial skin images (top) and tomographic keratinocyte architecture (bottom left: top layer of epidermal keratinocytes, right: top four layers of spatial epidermal keratinocyte architecture) in young [age 25 (A)], middle-aged [age 46 (B)], and elderly subjects [age 65 (C)].

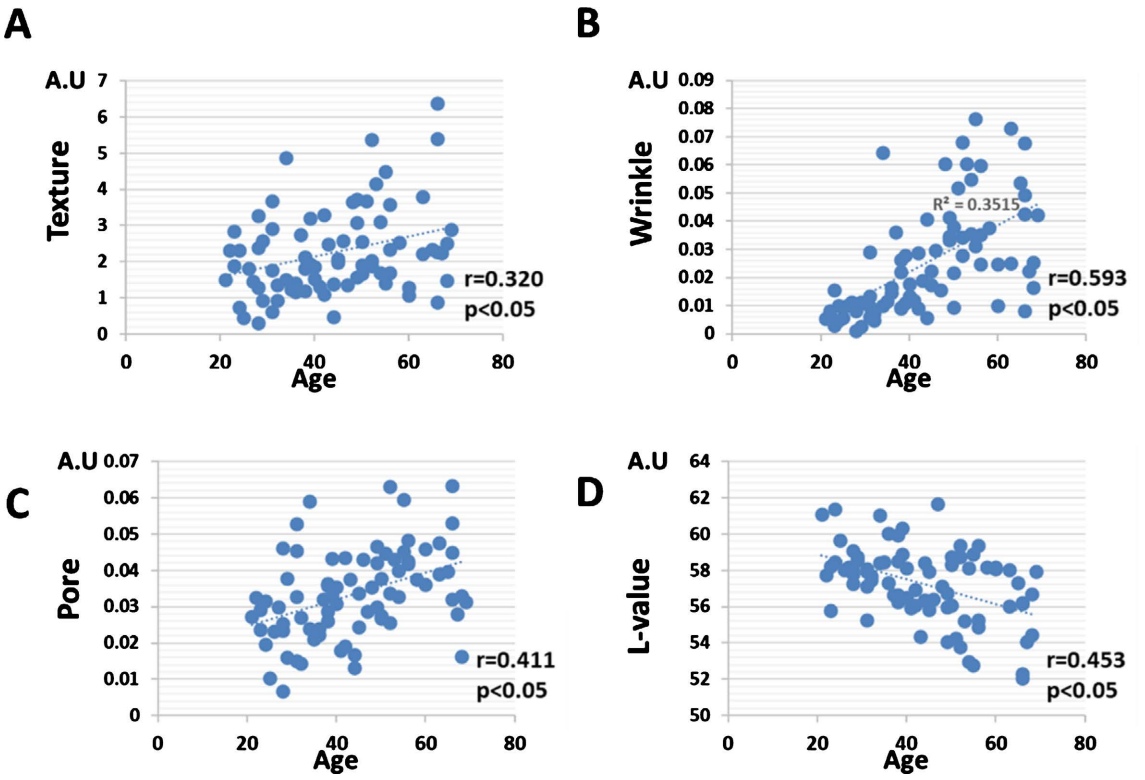

Figure 6. Age-related alterations of texture (A), wrinkles (B), pores (C), and L-value (D).

Notably, the cellular density showed significant correlations with skin hydration (Figure 7(A)), TEWL (Figure 7(B)), texture (Figure 7(C)), wrinkles (Figure 7(D)), pores (Figure 7(E)), and L value (Figure 7(F)).

The cellular uniformity was also significantly associated with each aging pa-

rameter, namely, skin hydration (Figure 8(A)), TEWL (Figure 8(B)), texture (Figure 8(C)), wrinkles (Figure 8(D)), pores (Figure 8(E)), and L value (Figure 8(F)).

The highly significant relationship among visual aging parameters and tomographic architecture allowed us to estimate the *in vivo* cellular architecture from

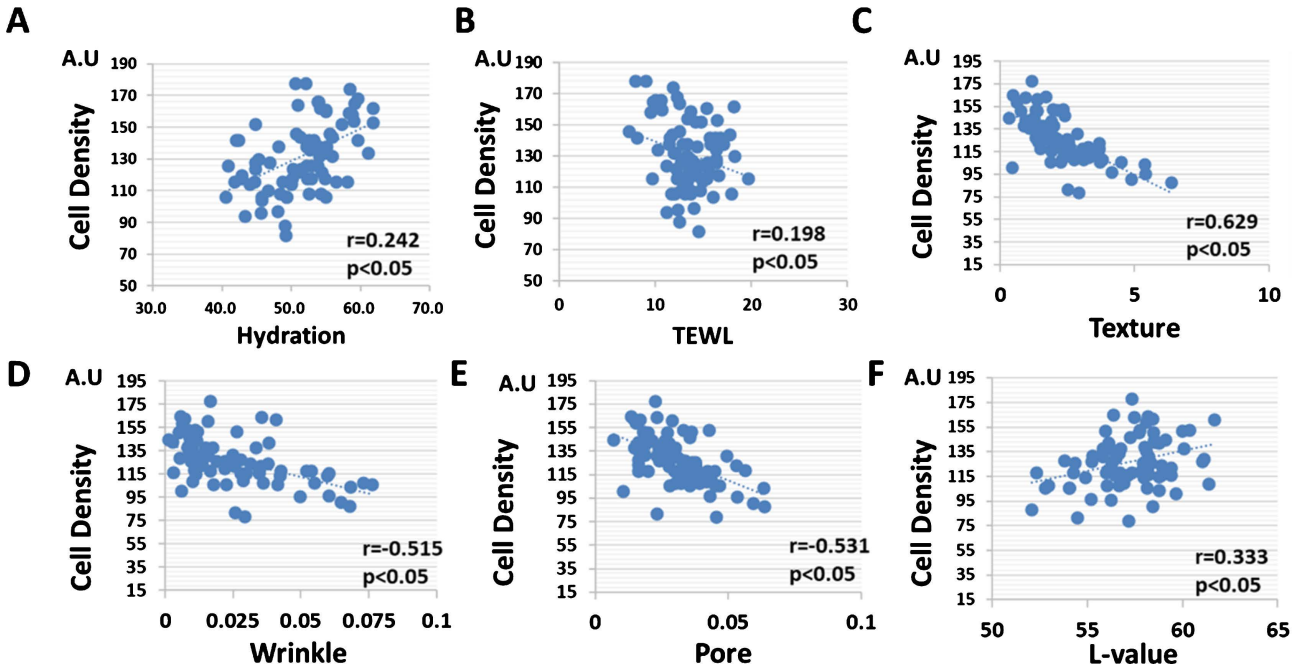

Figure 7. Significant correlations of cell density with hydration (A), TEWL (B), texture (C), wrinkles (D), pores (E), and L-value (F).

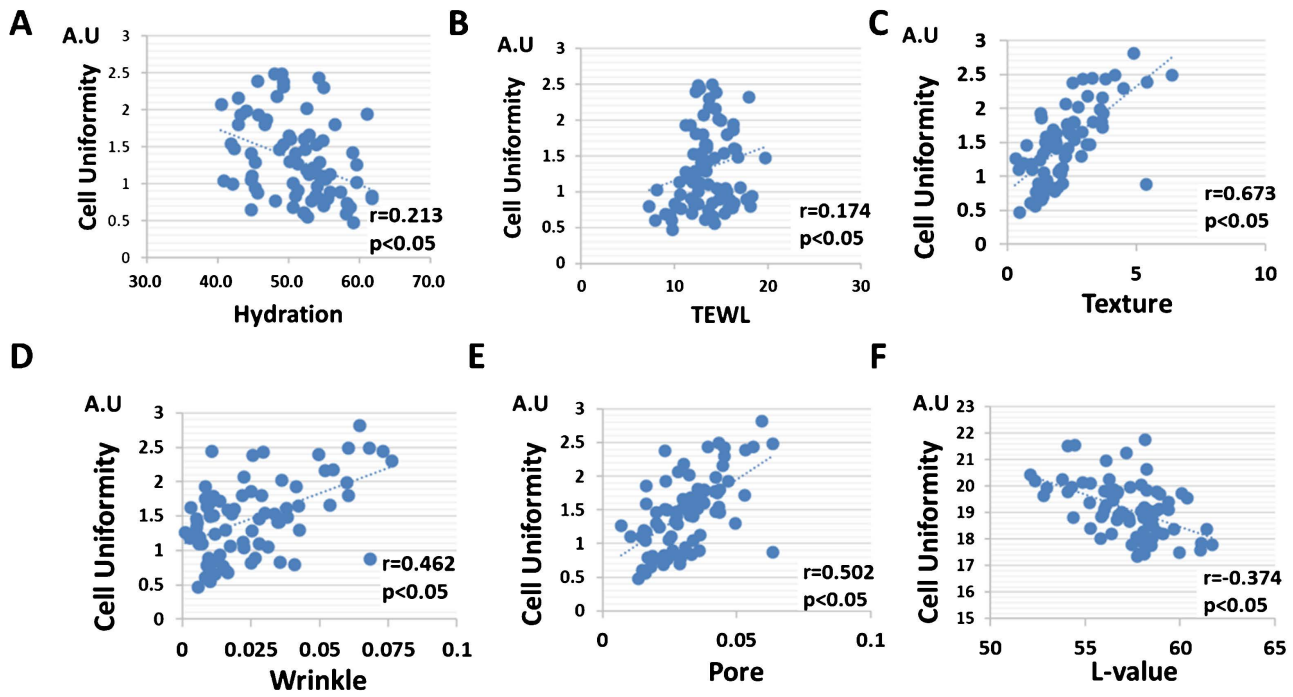

Figure 8. Significant correlations of cell uniformity with hydration (A), TEWL (B), texture (C), wrinkles (D), pores (E), and L-value (F).

visual parameters. Using regression analysis, we established the following formulae:

Estimated keratinocyte density (Number of cells/space) = −13.3002 × Texture Score + 363.6159 × Pore Score − 78.3089 × Wrinkle score − 0.005611 × L (lightness) score + 223.5498

Estimated keratinocyte uniformity = 0.1444 × Texture Score + 3.7958 × Pore Score + 7.4499 × Wrinkle score − 0.03147 × L (lightness) score + 2.6077

According to the formulae, the estimated keratinocyte density and estimated keratinocyte uniformity showed highly significant correlations with architectural density and uniformity, respectively (Figure 9).

Skin cell interconnectivity parameter

Cell density and cell uniformity were also merged into a single parameter that represents tomographic architecture, which we call skin cell interconnectivity. This parameter was calculated by adding the fit-scale from 0 to 1 of cell density and the reversed fit-scale from 0 to 1 of cell uniformity from the database established in this study. In this way, a higher score of the skin cell interconnectivity parameter represents higher cell density and more uniform cells, in terms of the tomographic cell architecture. There was a high positive correlation between cell density and cell interconnectivity, and a high negative correlation between cell uniformity and cell interconnectivity (Figure 10(A), Figure 10(B)). Skin cell interconnectivity was also estimated from visible skin aging parameters by using regression analysis, which demonstrated a highly significant correlation (Figure 10(C)).

3.2. Reversal of Skin Architectural Aging by Application of SK-II

We next examined whether treatment with SK-II improves the architectural aging. Compared with that in the untreated control area in the right forearm, the application of SK-II on the left forearm significantly improved skin hydration (Figure 11(A)) and TEWL (Figure 11(B)), even after 2 weeks of treatment. In parallel with the improvement of skin moisture, SK-II significantly increased the cellular density and decreased the cellular uniformity after 2 and 4 weeks of application, compared with the findings in the untreated control area (Figure 11(C), Figure 11(D), and Figure 12).

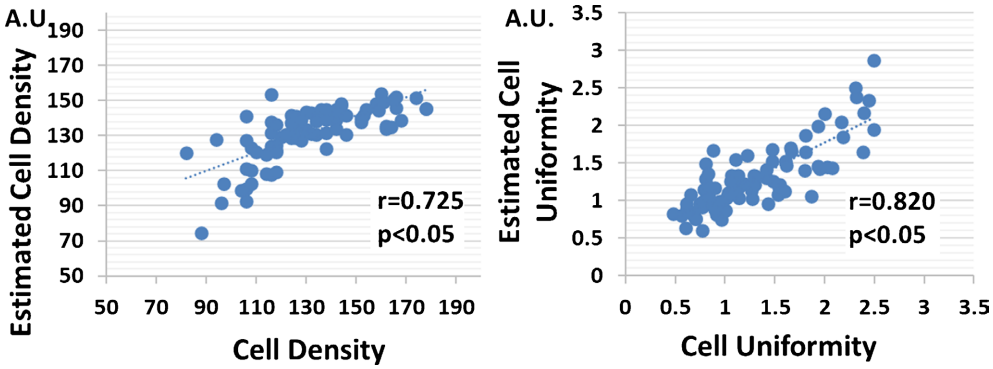

Figure 9. High correlation between cell density and estimated cell density (A), and between cell uniformity and estimated cell uniformity (B).

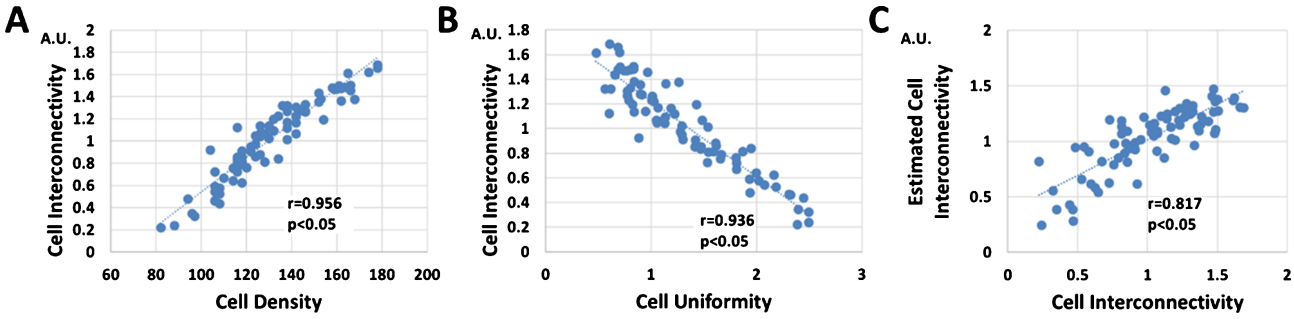

Figure 10. High correlations between cell density and cell interconnectivity (A), between cell uniformity and cell interconnectivity (B), and between cell interconnectivity and estimated cell interconnectivity (C).

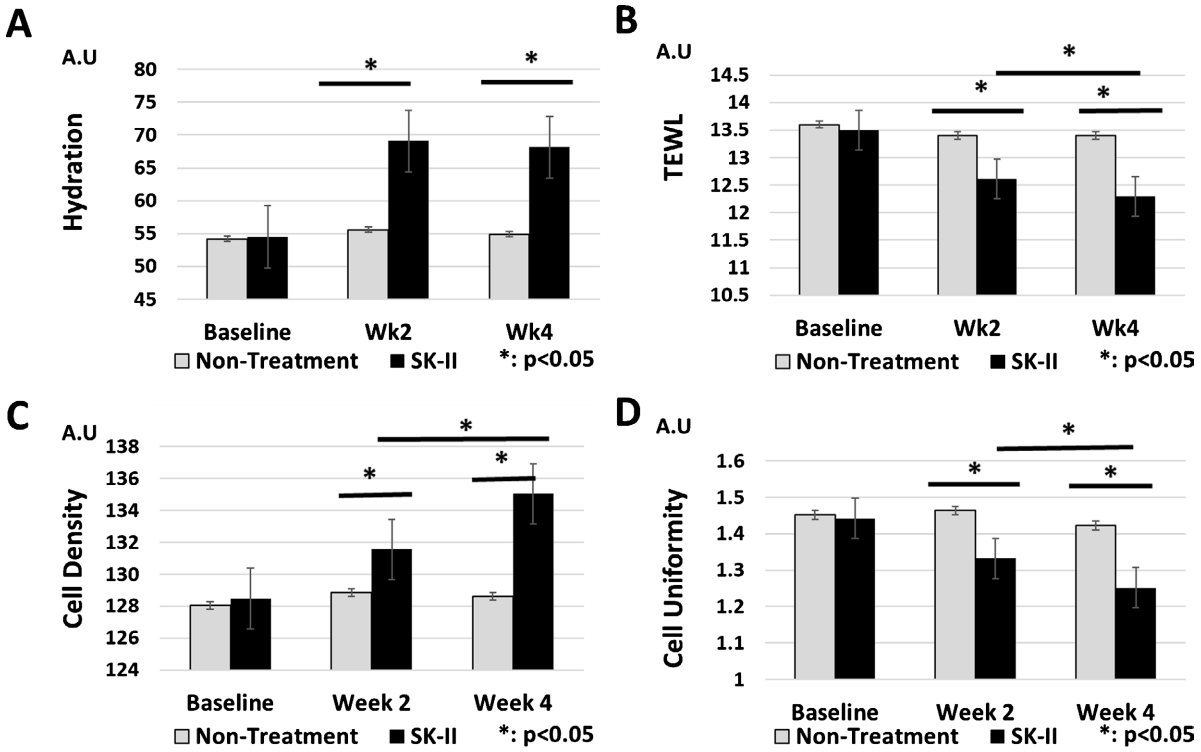

Figure 11. Improvements of hydration (A), TEWL (B), cell density (C) and cell uniformity (D) by topical treatment with SK-II compared with those in the untreated control (NT).

3.3. Reversal of Visual Facial Aging by Application of SK-II

As SK-II rejuvenated the architectural keratinocyte aging in the forearm as early as at 2 weeks of daily application, we next examined whether its treatment reverses the facial aging parameters earlier than 2 weeks. SK-II was applied twice daily on the face in 35 women and the facial aging parameters were assessed at baseline (day 0) and on 3, 7, and 14 days after its application. As shown in Table 1, the treatment with SK-II significantly improved all facial skin aging parameters: hydration, TEWL, texture, wrinkles, pores, and L value, compared with the findings at baseline, as early as at day 3. The rejuvenating effects of SK-II became even more pronounced at days 7 and 14 compared with those at day 3 (Table 1).

In addition, the estimated keratinocyte density, estimated keratinocyte un-

iformity and estimated skin cell interconnectivity were significantly and time-dependently rejuvenated by daily treatment with SK-II (Figure 13 and Figure 14).

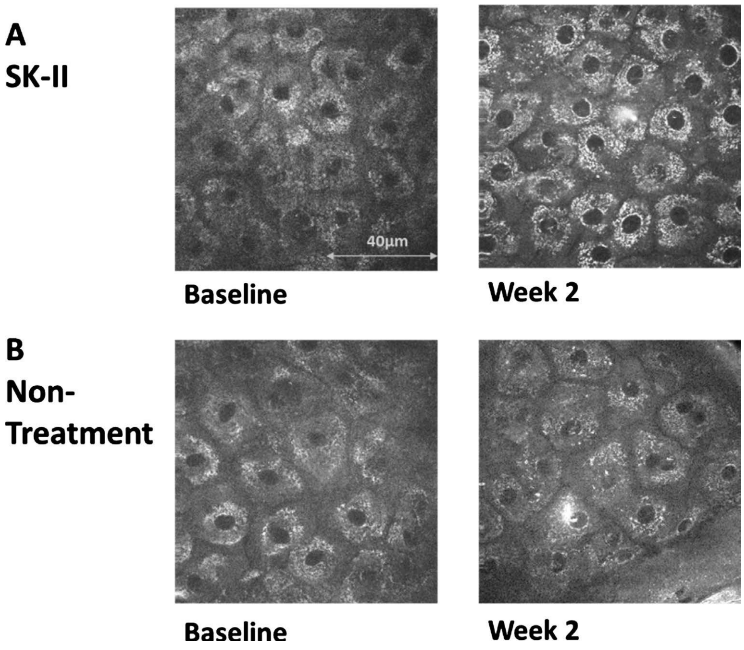

Figure 12. Example images of tomographic keratinocyte architecture upon topical treatment with SK-II at baseline (top left) and week 2 (top right) (A), and in the untreated control at baseline (bottom left) and week 2 (bottom right).

Table 1. Improvement of facial skin aging parameters by SK-II application.

	Hydration	TEWL	Texture	Wrinkles	Pores	L value
Baseline	60.18 ± 7.435	13.76 ± 5.0867	2.204 ± 1.1383	0.0477 ± 0.0063	0.0185 ± 0.0039	59.74 ± 4.3844
Day 3	67.33 ± 7.879*	12.69 ± 4.9914*	2.001 ± 1.0899*	0.0387 ± 0.0061*	0.0164 ± 0.0033*	60.03 ± 4.5213*
Day 7	70.47 ± 7.441*†	11.45 ± 4.4099*†	1.824 ± 1.0133*†	0.0348 ± 0.0055*†	0.0155 ± 0.0030*†	60.19 ± 4.2878*†
Day 14	71.64 ± 6.913*†	11.04 ± 4.7213*†	1.821 ± 1.4341*†	0.0345 ± 0.0057*†	0.0151 ± 0.0034*†	60.21 ± 4.3238*†

*: Significant difference from baseline ($P < 0.05$), †: Significant difference from day 3 ($P < 0.05$).

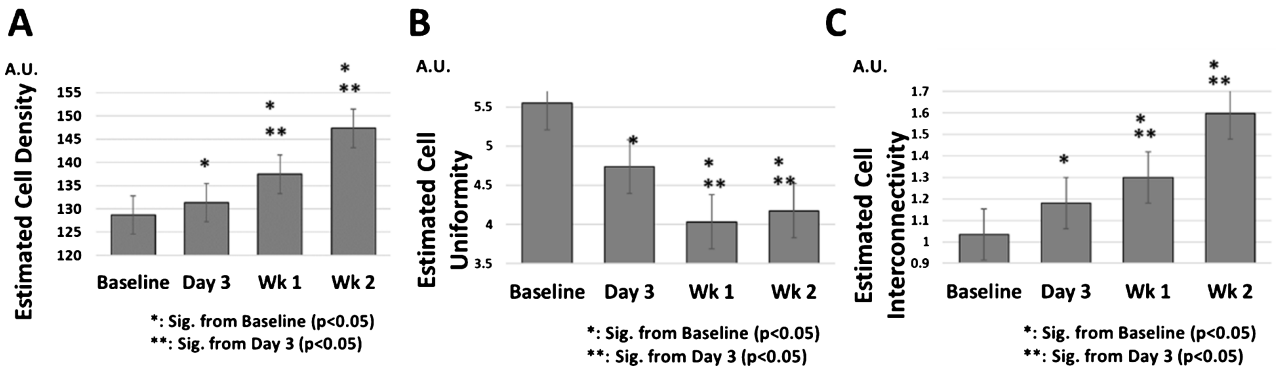

Figure 13. Improvements of estimated cell density (A), estimated cell uniformity (B) and estimated skin cell interconnectivity (C) by topical treatment with SK-II compared with the baseline.

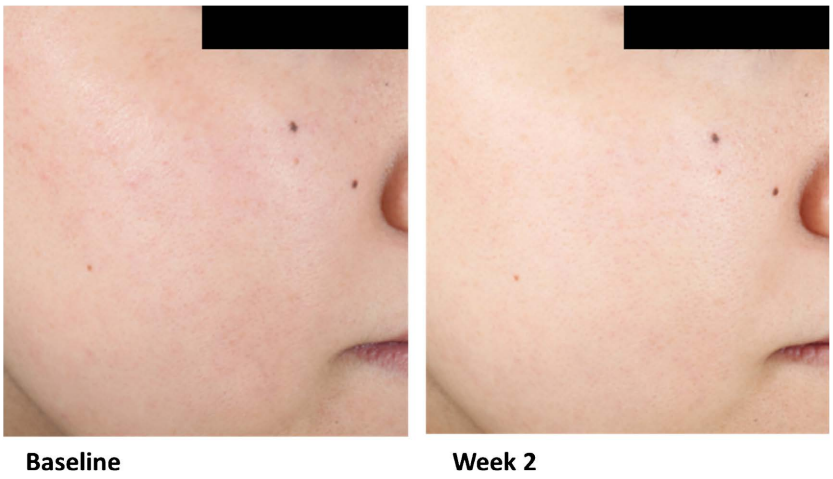

Figure 14. Example facial skin images at baseline (left) and after 2 weeks of topical treatment with SK-II.

4. Discussion

Rejuvenation of facial skin aging is a general concern in humans. Over the course of aging, facial skin gradually acquires visual signs of aging including a rough texture, wrinkles, pore dilation, and dull skin tone in association with dehydration [7] [18] [19] [20] [21] [22].

In the present study, we analyzed the spatial architecture of keratinocytes *in vivo* using non-invasive two-photon tomography in terms of spatial biology and demonstrated that facial skin aging was correlated with decreased keratinocyte density and increased keratinocyte uniformity in female subjects of various ages. Notably, the architectural cellular aging was also significantly associated with each visual aging parameter, namely, rough texture, wrinkles, pore dilation, and dull skin tone. These results suggested that visual facial skin aging is strongly interconnected with architectural cellular aging. The high interconnectivity between visual and architectural parameters allowed us to successfully develop formulae to estimate the architectural keratinocyte density and uniformity from the visual aging parameters of rough texture, wrinkles, pore dilation, and dull skin tone.

In addition, the architectural cellular aging parameter was correlated with facial dehydration due to aging. As some subjects showed youthful facial parameters, we assumed that the appropriate application of effective moisturizer might reverse the aging process. This was indeed the case. SK-II significantly improved the visual facial skin aging parameters during 2 weeks of twice-daily application in concert with increased skin hydration. It also significantly reversed the architectural cellular aging parameters as a demonstration of a new trajectory of anti-aging effects.

SK-II is a potent moisturizing GFF-containing skin care product [8] [15] [16]. GFF is known to activate the aryl hydrocarbon receptor and upregulate the expression of skin barrier-related proteins [10] [11] [12] [13]. It also increases the

production of the anti-inflammatory cytokine interleukin-37 in epidermal keratinocytes [23]. In addition, GFF inhibits oxidative stress by activating the cellular antioxidative system [11] [14]. These multifaceted properties of GFF may facilitate its moisturizing and anti-inflammaging effects [23] [24] [25]. These biological effects may underpin the anti-aging effects of SK-II.

There are several limitations of this study, which should be mentioned here. The subcellular mechanisms by which SK-II improves the various aging parameters remain unclear. Further longitudinal prospective study is necessary to elucidate whether the GFF-containing skin care product is capable of decelerating the long-term aging process.

In conclusion, the keratinocyte cellular architecture (density, uniformity and skin interconnectivity) is a useful aging parameter for the broadly utilization of skin aging research, which is interconnected with visual and physiological aging parameters. In addition, the continuous application of SK-II may contribute to maintaining a youthful facial appearance.

Author Contributions

Conceptualization and clinical investigation were performed by K.M., Y.M., K.F., and C.F. K.M., S.S.., and M.F. wrote the first draft of the manuscript, while all authors revised it. All authors have read and agreed to the published version of the manuscript.

Funding

This research received no external funding.

Institutional Review Board Statement

This study was conducted in accordance with the tenets of the Declaration of Helsinki and approved by P&G Ethics Committee. Data acquisition and analysis were performed in compliance with protocols approved by the Ethical Committee of Global Product Stewardship in P&G Innovation Godo Kaisya (ethical approval numbers CT12002, CT12006, and CT23002). Written informed consent was obtained from all participants prior to inclusion in the study.

Informed Consent Statement

Informed consent was obtained from all subjects involved in the study.

Data Availability Statement

The data presented in this paper are available on request from the corresponding author. The data are not publicly available because of privacy restrictions.

Acknowledgments

We thank Kiriko Ishida, Yasuko Inoue, and Yoko Munakata for help with the facial clinical study (Studies 1 and 3), and Denny Deng for help with the Chinese

female study (Study 2) and facial imaging.

Conflicts of Interest

The authors declare no conflicts of interest regarding the publication of this paper.

References

[1] Chin, T., Lee, X.E., Ng, P.Y., Lee, Y. and Dreesen, O. (2023) The Role of Cellular Senescence in Skin Aging and Age-related Skin Pathologies. *Frontiers in Physiology*, **14**, Article 1297637. https://doi.org/10.3389/fphys.2023.1297637

[2] Liao, Y.H., Chen, S.Y., Chou, S.Y., Wang, P.H., Tsai, M.R. and Sun, C.K. (2013) Determination of Chronological Aging Parameters in Epidermal Keratinocytes by *in Vivo* Harmonic Generation Microscopy. *Biomedical Optics Express*, **4**, 77-88. https://doi.org/10.1364/BOE.4.000077

[3] Akazaki, S., Nakagaa, H., Kazama, H., Osanai, O., Kawai, M., Takema, Y. and Imokawa, G. (2002) Age-Related Changes in Skin Wrinkles Assessed by a Novel Three-Dimensional Morphometric Analysis. *British Journal of Dermatology*, **147**, 689-695. https://doi.org/10.1046/j.1365-2133.2002.04874.x

[4] Kakudo, N., Kushida, S., Tanaka, N., Minakata, T., Suzuki, K. and Kusumoto, K. (2011) A Novel Method to Measure Conspicuous Facial Pores Using Computer Analysis of Digital-Camera-Captured Images: The Effect of Glycolic Acid Chemical Peeling. *Skin Research and Technology*, **17**, 427-433. https://doi.org/10.1111/j.1600-0846.2011.00514.x

[5] Miyamoto, K., Takiwaki, H., Hillebrand, G.G. and Arase, S. (2002) Development of a Digital Imaging System for Objective Measurement of Hyperpigmented Spots on the Face. *Skin Research and Technology*, **8**, 227-235. https://doi.org/10.1034/j.1600-0846.2002.00325.x

[6] Takiwaki, H. (2002) Instrumental Quantification and Its Clinical Application in the Future. *Skin Research and Technology*, **8**, 71-72. https://doi.org/10.1034/j.1600-0846.2002.00344.x

[7] Miyamoto, K., Inoue, Y., Hsueh, K., Liang, Z., Yan, X., Yoshii, T. and Furue M. (2011) Characterization of Comprehensive Appearances of Skin Ageing: An 11-Year Longitudinal Study on Facial Skin Ageing in Japanese Females at Akita. *Journal of Dermatological Science*, **64**, 229-236. https://doi.org/10.1016/j.jdermsci.2011.09.009

[8] Miyamoto, K., Dissanayake, B., Wanigasekara, S., Fujii, K., Yan, X. and Furue, M. (2023) Expanded Follicle-Sulcus-Crack Complex Is an Early Warning Sign of Facial Skin Aging: Improvement by Application of *Galactomyces* Ferment Filtrate-Containing Skin Product. *Journal of Cosmetics, Dermatological Sciences and Applications*, **13**, 91-106. https://doi.org/10.4236/jcdsa.2023.132010

[9] Miyamoto, K., Inoue, Y., Yan, X., Yagi, S., Suda, S. and Furue, M. (2023) Significant Reversal of Facial Wrinkle, Pigmented Spot and Roughness by Daily Application of Galactomyces Ferment Filtrate-Containing Skin Products for 12 Months—An 11-Year Longitudinal Skin Aging Rejuvenation Study. *Journal of Clinical Medicine*, **12**, Article 1168. https://doi.org/10.3390/jcm12031168

[10] Takei, K., Mitoma, C., Hashimoto-Hachiya, A., Takahara, M., Tsuji, G., Nakahara, T. and Furue, M. (2015) Galactomyces Fermentation Filtrate Prevents T Helper 2-Mediated Reduction of Filaggrin in an Aryl Hydrocarbon Receptor-Dependent

Manner. *Clinical and Experimental Dermatology*, **40**, 786-793. https://doi.org/10.1111/ced.12635

[11] Hashimoto-Hachiya, A., Tsuji, G. and Furue, M. (2019) Antioxidants Cinnamaldehyde and Galactomyces Fermentation Filtrate Downregulate Senescence Marker CDKN2A/p16INK4A via NRF2 Activation in Keratinocytes. *Journal of Dermatological Science*, **96**, 53-56. https://doi.org/10.1016/j.jdermsci.2019.09.002

[12] Wong, W.R., Hakozaki, T., Yoshii, T., Chen, T.Y. and Pan, J.H.S. (2011) Up-Regulation of Tight Junction-Related Proteins and Increase of Human Epidermal Keratinocytes Barrier Function by Saccharomycosis Ferment Filtrate. *Journal of Cosmetics, Dermatological Sciences and Applications*, **1**, 15-24. https://doi.org/10.4236/jcdsa.2011.11003

[13] Kataoka, S., Hattori, K., Date, A. and Tamura, H. (2013) Human Keratinocyte Caspase-14 Expression Is Altered in Human Epidermal 3D Models by Dexamethasone and by Natural Products Used in Cosmetics. *Archives of Dermatological Research*, **305**, 683-689. https://doi.org/10.1007/s00403-013-1359-0

[14] Furue, M., Uchi, H., Mitoma, C., Hashimoto-Hachiya, A., Chiba, T., Ito, T., Nakahara, T. and Tsuji, G. (2017) Antioxidants for Healthy Skin: The Emerging Role of Aryl Hydrocarbon Receptors and Nuclear Factor-Erythroid 2-Related Factor-2. *Nutrients*, **9**, Article 223. https://doi.org/10.3390/nu9030223

[15] Miyamoto, K., Dissanayake, B., Omotezako, T., Takemura, M., Tsuji, G. and Furue, M. (2021) Daily Fluctuation of Facial Pore Area, Roughness and Redness among Young Japanese Women; Beneficial Effects of Galactomyces Ferment Filtrate Containing Antioxidative Skin Care Formula. *Journal of Clinical Medicine*, **10**, Article 2502. https://doi.org/10.3390/jcm10112502

[16] Miyamoto, K., Munakata, Y., Yan, X., Tsuji, G. and Furue, M. (2022) Enhanced Fluctuations in Facial Pore Size, Redness, and TEWL Caused by Mask Usage Are Normalized by the Application of a Moisturizer. *Journal of Clinical Medicine*, **11**, Article 2121. https://doi.org/10.3390/jcm11082121

[17] Miyamoto, K. and Kudoh, H. (2013) Quantification and Visualization of Cellular NAD(P)H in Young and Aged Female Facial Skin with *in Vivo* Two-photon Tomography. *British Journal of Dermatology*, **169**, 25-31. https://doi.org/10.1111/bjd.12370

[18] Pena, A.M., Baldeweck, T., Decenciere, E., Koudoro, S., Victorin, S., Raynaud, E., Ngo, B., Bastien, P., Brizion, S. and Tancrede-Bohin, E. (2022) *In Vivo* Multiphoton Multiparametric 3D Quantification of Human Skin Aging on Forearm and Face. *Scientific Reports*, **12**, Article No. 14863. https://doi.org/10.1038/s41598-022-18657-z

[19] Zhang, Y., Liu, X., Wang, J., Du, L., Ma, Y., Liu, W., Ye, R., Yang, Y. and Xu, H. (2022) Analysis of Multi-Part Phenotypic Changes in Skin to Characterize the Trajectory of Skin Aging in Chinese Women. *Clinical, Cosmetic and Investigational Dermatology*, **15**, 631-642. https://doi.org/10.2147/CCID.S349401

[20] Campiche, R., Trevisan, S., Seroul, P., Rawlings, A.V., Adnet, C., Imfeld, D. and Voegeli, R. (2019) Appearance of Aging Signs in Differently Pigmented Facial Skin by a Novel Imaging System. *Journal of Cosmetic Dermatology*, **18**, 614-627. https://doi.org/10.1111/jocd.12806

[21] Cho, C., Lee, E., Park, G., Cho, E., Kim, N., Shin, J., Woo, S., Ha, J. and Hwang, J. (2022) Evaluation of Facial Skin Age Based on Biophysical Properties *in Vivo*. *Journal of Cosmetic Dermatology*, **21**, 3546-3554. https://doi.org/10.1111/jocd.14653

[22] Flament, F., Jacquet, L., Ye, C., Amar, D., Kerob, D., Jiang, R., Zhang, Y., Kroely, C., Delaunay, C. and Passeron, T. (2022) Artificial Intelligence Analysis of over Half a Million European and Chinese Women Reveals Striking Differences in the Facial Skin Ageing Process. *The Journal of the European Academy of Dermatology and Venereology*, **36**, 1136-1142. https://doi.org/10.1111/jdv.18073

[23] Yan, X., Tsuji, G., Hashimoto-Hachiya, A. and Furue, M. (2022) Galactomyces Ferment Filtrate Potentiates an Anti-Inflammaging System in Keratinocytes. *Journal of Clinical Medicine*, **11**, Article 6338. https://doi.org/10.3390/jcm11216338

[24] Tsuji, G., Hashimoto-Hachiya, A., Matsuda-Taniguchi, T., Takai-Yumine, A., Takemura, M., Yan, X., Furue, M. and Nakahara, T. (2022) Natural Compounds Tapinarof and Galactomyces Ferment Filtrate Downregulate IL-33 Expression via the AHR/IL-37 Axis in Human Keratinocytes. *Frontiers in Immunology*, **13**, Article 745997. https://doi.org/10.3389/fimmu.2022.745997

[25] Nakajima, A., Sakae, N., Yan, X., Hakozaki, T., Zhao, W., Laughlin, T. and Furue, M. (2022) Transcriptomic Analysis of Human Keratinocytes Treated with Galactomyces Ferment Filtrate, a Beneficial Cosmetic Ingredient. *Journal of Clinical Medicine*, **11**, Article 4645. https://doi.org/10.3390/jcm11164645